

1 **Nonlinear Dynamics of seismicity and fault zone strain around large dam: the case of Enguri**
2 **dam, Caucasus.**

3 T. Chelidze, T. Matcharashvili, V. Abashidze, N. Dovgal, E. Mepharidze, L. Chelidze

4 M. Nodia Institute of Geophysics, Tbilisi State University, Tbilisi, Georgia

5 **Abstract**

6 The 271 m high Enguri arch dam, still one of the highest arch dam in operation in the world, was
7 built in the canyon of the Enguri river (West Georgia) in the 1970s. It is located in a zone of high
8 seismicity (MSK intensity IX) and close to the Ingirishi active fault. The high seismic and
9 geodynamical activities together with the large number of people living downstream of the dam
10 made the Enguri dam a potential source of a major catastrophe in Georgia. Thus, the Enguri Dam
11 with its 1 billion cubic meters water reservoir should be under permanent monitoring. At the same
12 time this area is an amazing natural laboratory, where one can investigate both tectonic and
13 geotechnical strains/processes and their response to the lake load-unload impact, i.e. the reaction to a
14 controllable loading of Earth crust. This is an important scientific issue, connected with a
15 fundamental problem of Reservoir Induces Earthquakes as well as with environmental geotechnical
16 problems, related to the safety of large dam. Application of nonlinear dynamics methods allows
17 dividing events, ordered by reservoir water regular strain impact from the background seismicity.
18

19 **1. Introduction.**

20 Monitoring of strains and seismic activity in the area of large dam is a unique tool for
21 understanding the intimate connections between earthquakes generation and man-made regular
22 quasi-periodic strains in the Earth, created by seasonal water load-unload in the reservoir. We can
23 consider large dams' area as a natural laboratory, providing possibility of studying seismic process
24 in almost controlled (repeated) conditions.

25 The 271 m high Enguri arc dam (still one of the largest in the world) was built in the canyon
26 of Enguri river in West Georgia. It is located close to the Ingirishi active fault system, in a zone of
27 high seismicity, MSK intensity IX. The volume of the lake at Enguri dam is 10^9 cubic meters and
28 the water level high in the lake varies seasonally by 100 m, which means that Enguri reservoir can
29 activate Reservoir-Triggered Seismicity (RTS). The dominant tectonic feature of the region is the
30 active East-West oriented Ingirishi fault, located to the north of the dam: its branch fault crosses the
31 foundation of the Enguri dam (Chelidze et al, 2013).

32 Taking into account high potential danger of the object, geophysical monitoring system was
33 organized even before construction works for providing secure exploitation of the large Enguri dam.
34 Due to a high seismic activity of the region, the seismic station's network was installed in the area of
35 Enguri dam also well before its construction with the aim of studying possible reservoir-triggered
36 activity (Balavadze, 1981). The monitoring system of Enguri Dam and its foundation includes
37 network of tiltmeters, piezometers and reverse plumbines in the dam body (Chelidze, 2013), meteo-
38 station, water level gauge for monitoring water level in the lake, as well as complex of strainmeter
39 and tiltmeters, installed in the dam body and its foundation (Abashidze, 2001).

40 The problem of human-induced earthquakes, including RTS, became quite actual last
41 decades (Grigoli et al, 2017; Foulger et al, 2017; Savage et al, 2017). The RTS pattern in the Enguri
42 area should depend on the Water Level (WL) variation regime in the lake (Gupta, 1992; Gupta,
43 2018). The main goal of the paper is to apply new methods of complexity analysis in order to assess
44 in a quantitative way the correlation between WL variations and local seismicity and define the scale
45 of man-made activity on the local (natural) seismicity pattern.

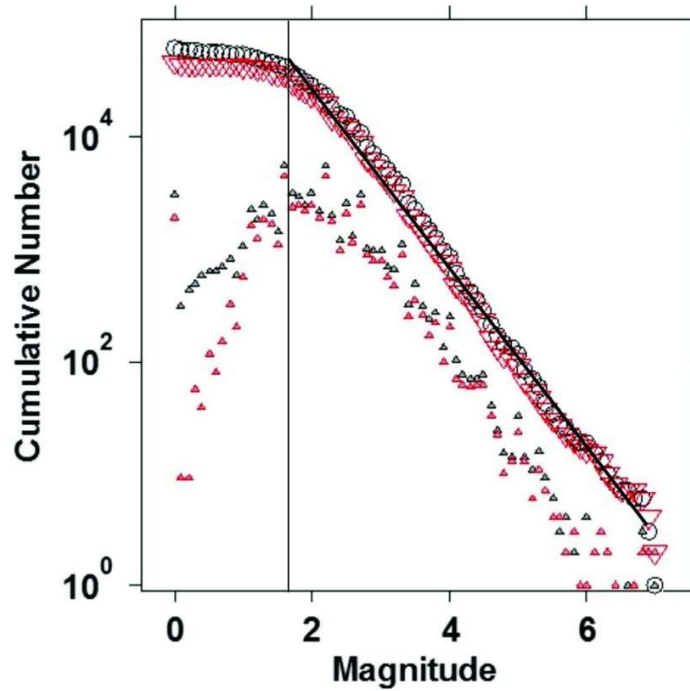
46 **2. Data.**

47 The branch fault of the main Ingirishi fault crosses the foundation of Enguri dam and thus,
48 poses hazard to its safety. In order to monitor permanently the fault behavior, two years before the
49 first filling of the reservoir, in December 1974, the quartz strainmeter, crossing the fault zone (FZ)
50 was installed in the adit, located 100 m downstream from the foundation of the dam. The
51 strainmeter's fixed and free parts are located on the intact rocks on the opposite sides of the FZ and
52 are separated from this 10 m-wide zone by the 5 m distance (the full length of the quartz tube is 22.5
53 m). This means that the device records displacement of the intact blocks, divided by the fault zone in
54 the normal to the fault plane direction, so it shows fault zone's extension/contraction. The free end
55 of the tube is equipped with photo-optical recording system (Abashidze, 2001). The displacements'
56 sensitivity of this system is of the order of 0.18 $\mu\text{m}/\text{mm}$, which allows also to record a tidal
57 component of the fault zone strain. At present, the laser system (Laser model R-39568, Green HeNe
58 Laser, 633 nm and Laser Position Sensor OBP-A-9L) doubles the photo-optical registration. The
59 laser is attached to the free end of the same quartz tube. Sensitivity of the strainmeter with the laser
60 sensor is one $\mu\text{m}/\text{mm}$.

61 The earthquake time series (ETS) for Enguri area from 3 January 1974 to 31 December 2016
62 was compiled using catalogs of Institute of Geophysics and International Seismological Centre. Our
63 study area includes events located on the distance 50 or 100 km from the lake. The completeness

64 magnitude (CM) for the whole used catalog is around M 1.7 (Fig. 1), but in some cases we confine
65 ourselves by magnitude 2.2 for confidence, as in some periods the CM value increased to M2.2 due
66 to non-stable functioning of national seismic network.

67



68

69 Fig. 1. Cumulative Gutenberg-Richter plot of the whole (black circles) and aftershock-depleted (downward
70 red triangles) catalogue of Georgia. The plot shows also the binned frequency-magnitude distribution of the
71 whole (upward black triangles) and aftershock-depleted (upward red triangles) catalogues. The
72 completeness magnitude is around M1.7.

73

74

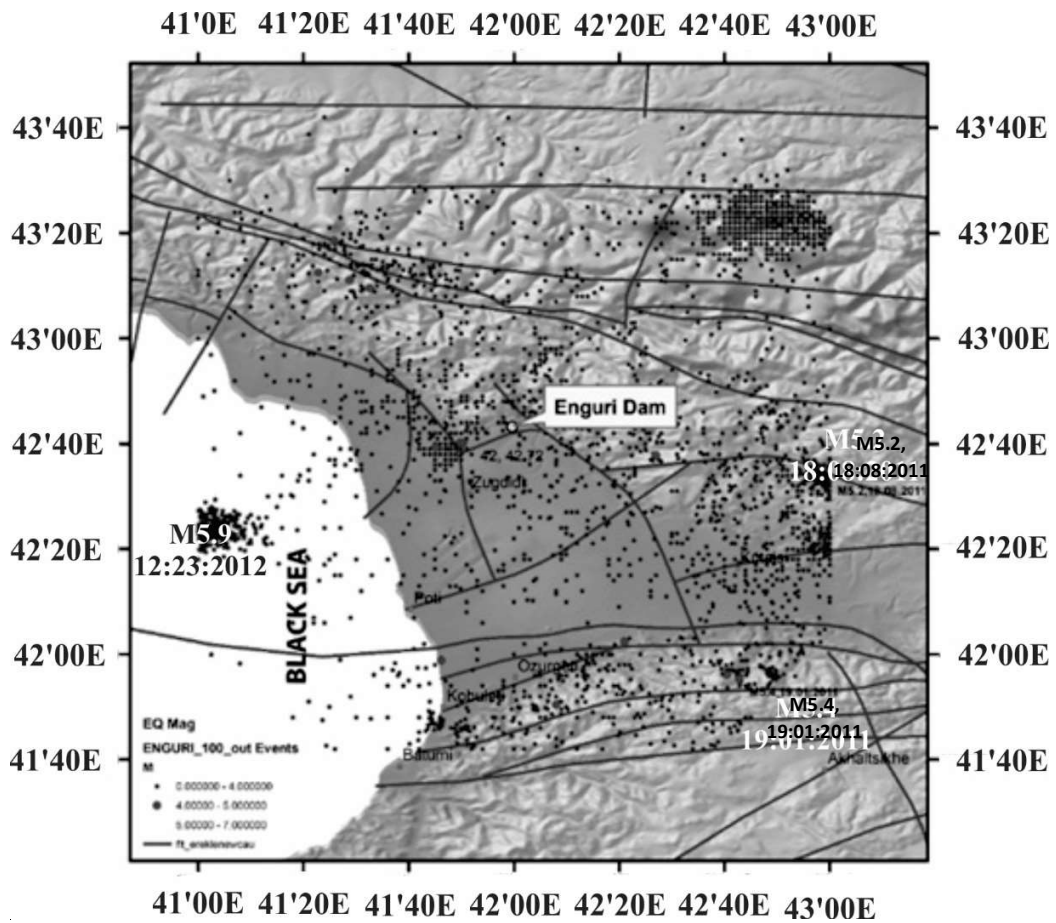
75

76

77

78

79



80

81 Fig. 2. Seismicity of the Enguri Dam region within 100 km distance with the scheme of active
 82 tectonic faults, according to (Gamkrelidze et al, 1998).

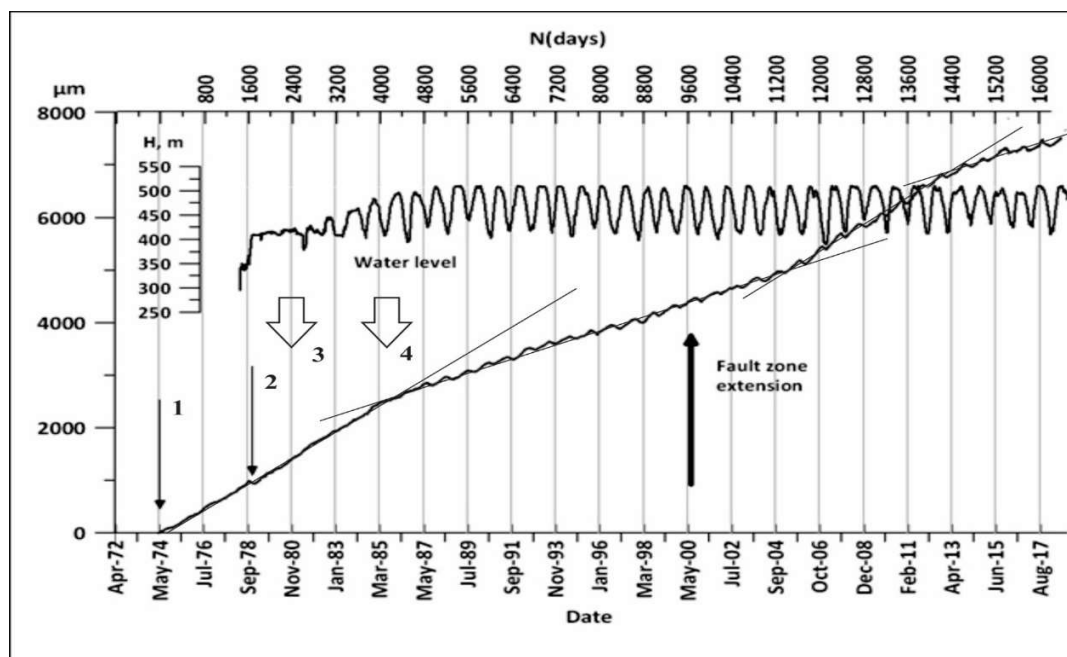
83

84 In Fig. 2 we present a spatial distribution of seismicity in the Enguri Dam region within 100
 85 km distance from the dam as well as the scheme of active tectonic faults, according to (Gamkrelidze
 86 et al, 1998).

87 Fig. 3 shows almost 40-years' history of the crossing the dam foundation fault zone
 88 extension - FZE - beginning from 1974 (i.e. FZE is variation of the normal to the fault plane
 89 displacement of the free end of the strainmeter) and water level (WL) change in the Enguri reservoir
 90 H beginning from April 1978. According to Fig 3 the dam area experiences stresses of different
 91 origin, acting on the different time scales, from decades to months and days. Actually, the object
 92 under study is a natural large-scale laboratory for investigation of geotectonic, man-made and
 93 environmental impacts on the fault zone deformation. The summary contributions of these processes
 94 are reflected in the time series of fault zone strain. It is evident that the fault dynamics reflects joint

95 influence of two main factors: one leads to piecewise linear (in time) displacement (trend
 96 component) and the other one – to quasiperiodic oscillations, decorating the main trend.

97 The long-term piecewise-linear trend documents persistent separation of fault faces (Fig. 3),
 98 extending to 7000 μm (7 mm) during observation period. The FZE rate (y) depends on the time (t)
 99 following a simple linear equation: $y(t) = at - b$. where the coefficient a , the slope of the linear
 100 component of the FZE or the strain rate, differs from one period to another (Table 1). As the trend
 101 component with the same strain rate was recorded even before dam construction and lake filling, we
 102 attribute it to the long-term regional tectonic stress action.
 103



104 Fig. 3. WL in the Enguri lake from 1978 (upper curve) to 2017 and the data on the
 105 extension/compaction of the branch of a large Ingirishi fault, crossing the foundation of the dam
 106 from 1974 to 2017 (lower curve). Arrow 1 corresponds to the start (in 1974) of strainmeter
 107 monitoring 4 years before impounding, arrow 2 – to the episode of the fault compaction by
 108 approximately 90 μm due to WL fast rising by 100 m in 1978, arrows 3 and 4 show the moments of
 109 transitions in the nonlinear dynamics pattern of local seismicity (see section 4). Upper horizontal
 110 axis shows number of days after start of strainmeter monitoring. Dashed straight lines mark periods
 111 of fault’s constant extension component slope.
 112

113 At the same time, the fault zone extension rate (FZER) changes significantly with time,
 114 reflecting action of some non-stationary factors. In the Table 1 we show the periodization of FZE

115 behavior following the pattern of data evolution according to Fig. 3, taking into consideration both
 116 components of strain – tectonic and anthropogenic.

117

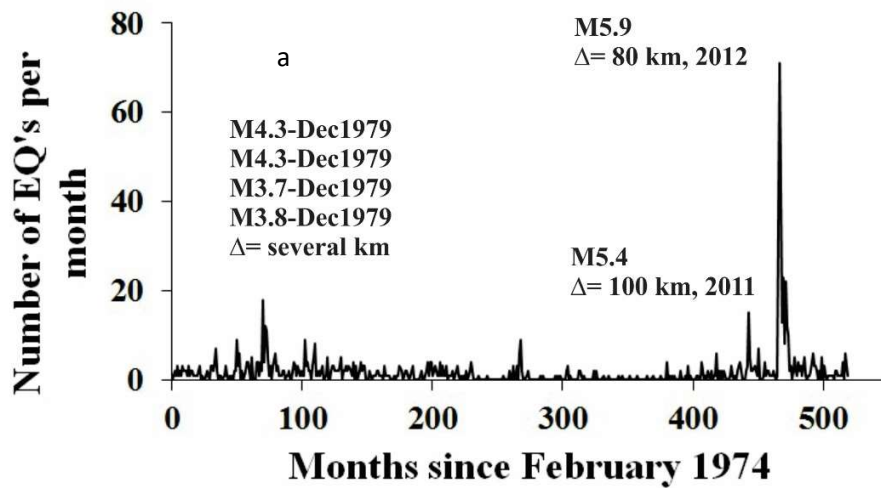
118 Table 1. Periodization of the fault zone extension

119

Number of periods	Periods	Number of days in the period; in brackets the same from the zero day (May 1974) to the end of the given period	Tectonic component of strain rate a microns/year	Pattern of lake impounding regime (man-made component of strain)
1	May1974–Jun 1978	1500 (1500)	250	Before lake impounding
2	Apr1978 –Jan 1981	1300 (2800)	235	WL in the lake raised to 100 m
3	Jan1981–May 1985	1400 (4200)	235	Irregular quasi-periodic regime
4	May 1985-Sep 2004	7000 (11200)	160	Regular quasi-periodic regime
5	Sep 2004–Feb 2013	3200 (14400)	230	Regular quasi-periodic regime
6	Feb 2013-Mar2018	2000 (16400)	150	Regular quasi-periodic regime

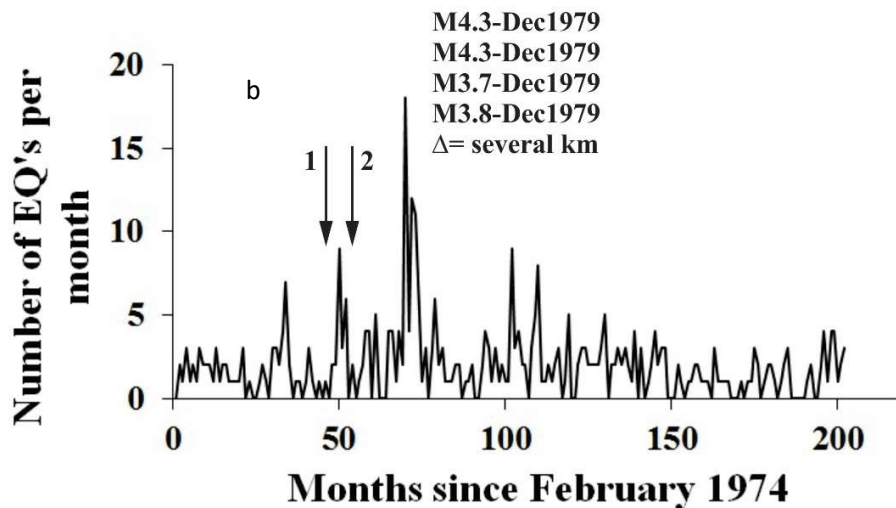
120

121 The most probable source of quasiperiodic changes in the FZE dynamics in Enguri area is
 122 the variation of the water load in the lake. We elucidate six periods with appreciable differences in
 123 the WL regime: i. May1974–Jun 1978, period before water fill, which we consider as a reference;
 124 ii. Apr1978–Jan 1981 is the period of the initial filling of reservoir; iii. Jan1981–May 1985 is the
 125 interval of initial irregular (quasiperiodic) variation of WL; iv. May 1985- Sep2004, in this period
 126 we observe regular quasi-periodic load-unload regime, though tectonic component of the strain rate
 127 varied in this period from 235 to 160 microns/year; v. during Sep 2004–Feb 2013 there is a regular
 128 quasi-periodic regime, but the tectonic component of the strain rate returns to the value 230
 129 microns/year; vi. in the interval Feb 2013-Mar2018 a quasi-periodic component is decorating the
 130 tectonic strain rate of 150 microns/year.



131

132



133

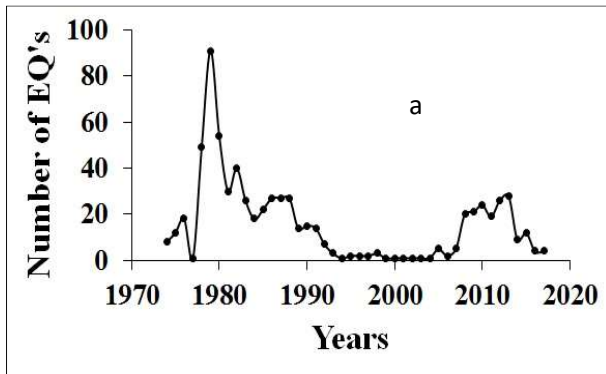
134 b.

135 Fig. 4 a, b. Number of EQs ($M \geq 2.2$) per month versus month number in the radius 100 km from the
 136 dam, Δ is the distance of from the epicenter of a given EQ to the dam: (a) since February 1974 till
 137 2017; (b) since February 1974 till 1991. Arrow marks 1 and 2 in Fig. 4 b correspond to: (1) beginning
 138 of filling and (2) -WL rising to 100 m high.

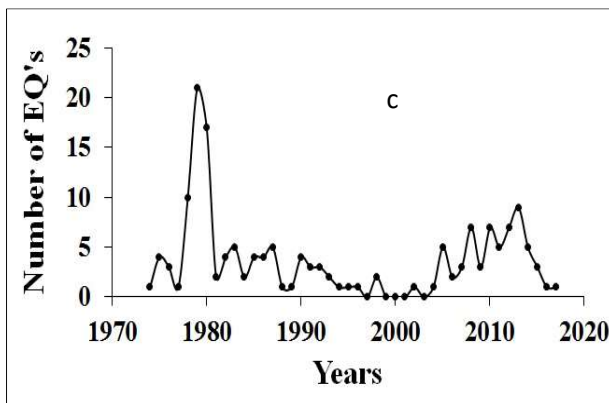
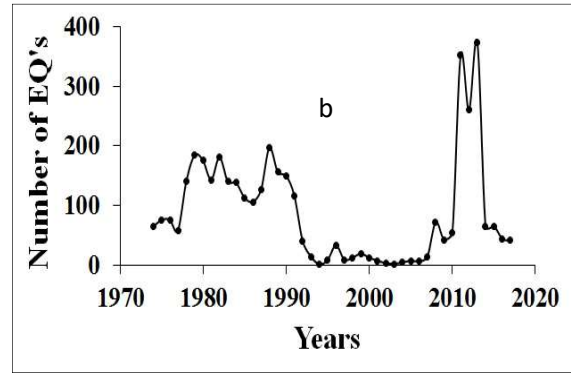
139

140 *General Characteristics of the test area seismicity.* In Fig. 4a we show the earthquake
 141 number per month from 1974 till 2017 and in Fig 4 (b) - the same on the extended time scale: since
 142 February 1976 till 1991 within 100 km distance from the dam. We also mark the magnitudes M and
 143 EQ's separation from the dam Δ for the strongest events. According to Fig. 5 b the strong seismic

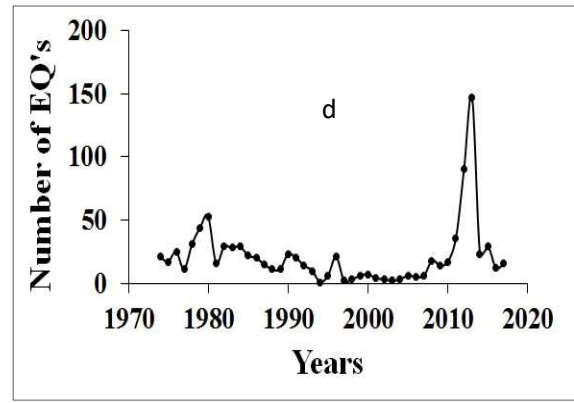
144 activity very close to the dam (Δ several km) in December 1979 with 4 events of magnitude M3.7-
 145 M4.3 follows the fast initial recharge of the lake to the critical for RTS initiation water level (100 m)
 146 in September 1978, i.e. with a lag 14 months.



147



148



149 Fig. 5. EQ number versus time in the near and larger zone: (a) EQ number - all events, including
 150 $M < 2.2$ in the near zone, $R = 50$ km; (b) EQ number - all events, including $M < 2.2$ in the large zone,
 151 $R = 100$ km; (c) EQ number – events with $M > 2.2$ in the near zone, $R = 50$ km; (d) EQ number –
 152 events with $M > 2.2$ in the large zone, $R = 100$ km.

153

154 Fig 4 a presents the number of events per month in the area with radiuses 50 and 100 km around
 155 Enguri dam, where several relatively strong EQs occur from 1974 to 2017. The epicenters of EQs
 156 M4.3 (21 Dec 1979), 4.3 (27 Dec 1979) are close to the Enguri lake and the EQs M5.4 (19 Jan
 157 2011), M5.9 (23 Dec 2012) shown in the Fig. 2a, lay on the distance 80-100 km.

158 To separate out more clearly the man-made impact, we present on the Fig. 5 b the detailed
 159 seismic rate during first 200 months after January 1974. The corresponding water level regime we

160 present in Fig. 3: the recharge began in April 1978 (arrow 1) and WL was abruptly risen to 100 m in
161 November 1978 (arrow 2). Almost simultaneously the abrupt compaction of the fault zone crossing
162 the foundation of dam by approximately $90 \mu\text{m}$ was registered by the strainmeter, installed on the
163 fault (Fig. 3). Almost the year later, in December 1979, series of EQs of magnitudes from 3.7 to 4.3
164 occur close to the reservoir. These effects follow (with an year lag) the time of WL rising to the
165 critical high of 100 m, when, according to existing data (Foulger, 2017; Gupta, 1992, 2018) the water
166 load can generate Reservoir Triggered Seismicity (RTS).

167 In order to better resolve the seismic events related to filling and exploitation of the dam
168 reservoir we used cellular approach (Kafka, John, 2011), namely, we plotted separately the time
169 sequences of all registered EQs (all EQs of magnitudes $M > 1$) in the near to dam zone, in the radius
170 $R = 50$ km from the dam and in the larger area, in the radius $R = 100$ km (Fig. 5 b). In Figs 5 c, d we
171 show the same data for the EQs of magnitudes $M \geq 2.2$. Considering Fig 5 we can conclude that the
172 EQ statistics in the near zone $R = 50$ km (Figs 5 a, c) is dominated by events connected with reservoir
173 impoundment and the swarm of EQs with Δ of the order of several km (compare with Fig. 4b), when
174 the most part of seismic activity in the larger zone $R = 100$ km (Figs 5 b, d) is due to the relatively
175 strong remote events of magnitude $M 5.2-5.9$ with Δ of the order of 80-100 km, which are too far
176 from Enguri dam and belong to the class of regional tectonic events (see Figs. 2, 3b). It follows that
177 in order to distinguish RIS events it is better to analyze seismic catalog in the near zone ($R = 50$ km),
178 where dominate seismic events, located close to Enguri dam. This restriction does not work for
179 analysis of complexity, especially when we analyze waiting times of EQ, because RIS is
180 characterized by quasiperiodic recurrence property due to regularity of reservoir load-unload. In turn
181 it means that the role of random seismic events when studying regularity in waiting times even at the
182 distance 100 km is relatively small.

183 **3. Methodology.**

184 The earthquake time series (ETS) presented in Fig. 5 a, b present a complex mix of
185 background seismicity, characteristic for the seismotectonics of the test area with a seismic response
186 to the lake impoundment and further – to WL quasiperiodic regulation. To single out the dynamical
187 patterns of the seismic data sets connected with WL variation, we used new effective methods of
188 complexity analysis (Chelidze, Valliantos, Telesca, Eds., 2018) applied to magnitudes and waiting
189 times of earthquake time series (ETS). The complexity analysis allow recognition of periods with
190 different level of ordering/determinism, which we connect with transition in WL regime from

191 disordered (1978-1984) to more ordered (1985-1986) and finally, to quasi-periodic loading (1986-
192 untill now). We give short description of these methods below.

193 Earlier several studies were devoted to complexity analysis of seismic regime in the Enguri
194 dam area, namely to variation of the phase diffusion coefficient of phase differences between daily
195 released seismic energy and water level daily variations (Matcharashvili et al, 2008; 2010),
196 Visibility Graph Analysis (Telesca, Chelidze, 2018) of Singular Spectrum Analysis (Telesca
197 et al, 2012). In the present paper we analyze recurrent patterns of local seismicity, using such
198 methods as Recurrence Plots, Detrended Fluctuation Analysis and Lempel and Ziv complexity
199 measure.

200 *Recurrence Plots (RP)* Recurrence Plots allow visualization of recurrent behavior of
201 dynamical system by plotting the arbitrary close (after some time lag) states in the two-dimensional
202 projection of the high-dimensional phase space trajectory (Eckmann et al, 1987; Webber and Marwan,
203 2015). The recurrence of the same state after some time lag is plotted on the square matrix, where
204 both axes represent time, by zeros and ones or by differently colored dots. The time lag between
205 recurrent points i and j of the trajectory is defined as the threshold time interval (threshold distance)
206 ε_i . The RP revealed some structural patterns, which are different for different degrees of determinism
207 in the phase space of the system.

208 *Detrended Fluctuation Analysis (DFA)*. Long-range time-correlations in the investigated data
209 sets were assessed by the method of Detrended Fluctuation Analysis (DFA) [Peng et al, 1994, 1995].
210 Method of DFA permits the detection of long-range correlations embedded in a nonstationary time
211 series through calculation of a quantitative parameter - DFA scaling exponent. This analysis technique
212 is widely accepted and often used for different types of time series including geophysical data sets
213 [e.g. Eichner, et al. 2003; Telesca, et al. 2004, 2007; Matcharashvii et al. 2012, 2015].

214 The basics of DFA are well known and described in series of often cited articles, so we will
215 just briefly stop on its main steps. At first given time series of N samples is integrated. After, the
216 integrated time series is divided into boxes of length n , and in each box the polynomial local trend is
217 calculated and removed. Then N/n mean squared residuals - Detrended Fluctuation Functions ($F(n)$),
218 should be calculated for each box of size n .

$$219 \quad F(n) = \sqrt{\frac{1}{N} \sum_{i=1}^N [Y(i) - Y_n(i)]^2}.$$

220 Since $F(n)$ increases with the box size n , in case of fractal or self-similar properties of analyzed data,
221 a power-law behavior $F(n) \sim n^\alpha$ can be revealed. If a power law scaling exists, the $F(n)$ vs. n

222 relationship, in double logarithmic fluctuation plot, will be linear or close to be linear and the scaling
223 exponent α can be estimated. If the scaling exponent $\alpha=0.5$, we deal with the uncorrelated dynamics
224 of random walk type [Peng et al. 1994; Liu et al 1999]. In this case, the time series is identical to white
225 noise. If α is different from 0.5, then the time series is regarded as long-range correlated or
226 anticorrelated, with $\alpha > 0.5$ or $\alpha < 0.5$ accordingly [Peng et al. 1994, 1995; Bahar et al 2001]. The
227 scaling exponent α is considered as an indicator of the nature of the fluctuations giving the information
228 about the long-range power law correlation properties in the analyzed data sets. DFA can be
229 accomplished for different order of the polynomial fitting in order to eliminate trends of certain origin.

230 *Recurrent quantification analysis.* In order to further quantify changes in dynamical structure
231 of analyzed data sets, we have used recurrence quantification analysis approach (Zbilut and Webber,
232 1992; Webber and Zbilut, 1994; et al., 2007; Webber and Marwan, 2015). In general RQA is a
233 quantitative extension of Recurrent Plot (RP) construction method which is based on the fact that
234 returns (recurrence) to the certain system condition or state space location is a fundamental property
235 of any dynamical system with quantifiable extent of determinism in underlying laws (Eckman et al.,
236 1987). In order RQA calculations to be successfully fulfilled, at first the phase space trajectory should
237 be reconstructed from the given scalar data sets, the proximity of points of the phase trajectory should
238 be tested and marked by the condition that the distance between them is less than a specified threshold
239 (Eckman et al., 1987). In this way, a two-dimensional representation of the recurrence features of
240 dynamics embedded in high-dimensional phase space can be obtained. Then small-scale structure of
241 recurrence plots can be quantified (Zbilut and Webber, 1992; Webber and Zbilut, 1994; Webber and
242 Zbilut, 2005; Marwan et al., 2007; Webber et al., 2009). RQA technique quantifies visual features in
243 a $N \times N$ distance matrix recurrence plot and defines several measures of complexity. Exactly, RQA
244 provides several measures of complexity based on the quantification of diagonally and vertically
245 oriented lines in the recurrence plot. In this research, we present one of such measures
246 (%Determinism), which often is used to reveal changes in the extent of regularity in analyzed data
247 sets.

248 *Lempel and Ziv complexity measure.* Lempel and Ziv algorithmic complexity (LZC)
249 calculation (Lempel & Ziv, 1976; Aboy et al. 2006; Hu and Gao, 2006) is another often used method
250 for quantification of the extent of order in analyzed data sets of different origin. LZC is based on the
251 transformation of given data sequence into new symbolic sequence. For this original data are
252 converted into a (0, 1) sequence by comparing them to a certain threshold value (usually median of
253 the original data set). Once the symbolic sequence is obtained, it is parsed to obtain distinct words,

254 and the words are encoded. Denoting the length of the encoded sequence for those words, the LZ
255 complexity can be defined as

$$256 \quad C_{LZ} = \frac{L(n)}{n}$$

257 where $L(n)$ is the length of the encoded sequence and n is the total length of sequence (Hu&Gao,
258 2006). Parsing methods can be different (Cover & Thomas, 1991; Hu and Gao, 2006). In this work
259 we used scheme described in Hu and Gao (2006). Data sequences with a certain regularity are less
260 complex, and the LZ complexity increases as the sequence grows in length and irregularity. In our
261 case the sequence length is constant and LZC depends only on the level of regularity.

262 **4. Results**

263 *Results of Complexity analysis.* In this study, we analyzed two types of ETS related to the
264 seismicity of Enguri area: the waiting times' and the magnitude sequences to study its changes
265 possibly linked with dynamical changes in the RTS characteristics of the investigated seismic area
266 related with the loading regime of the dam.

267 As we mentioned earlier, though the number of events in the far zone can be spoiled by the
268 EQs, not related to the reservoir-induced strain, the waiting times' (WT) distribution is less sensitive
269 to (background) random events even relatively far from the dam, i.e. for R=100 km.

270 *Results for the near zone R=50 km.* In this case (for R=50 km) we included into complexity
271 analysis, namely, RP and DFA methods, EQs below representative magnitude in order to fulfill the
272 condition of used methods – to have at least 500 events.

273

274

275

276

277

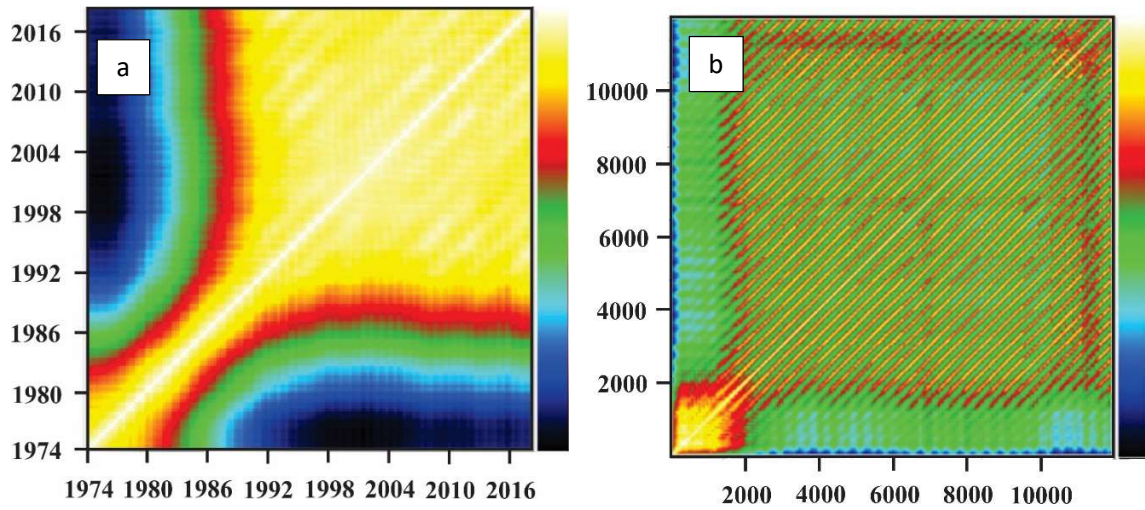
278

279

280

281

282



294

295

296

297

298

299

300

301

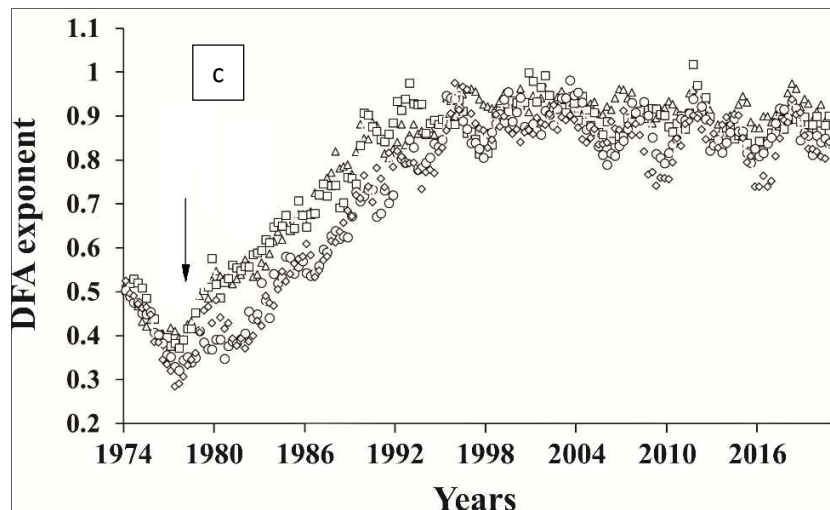
302

303

304

305

306



307

308

309

310

311

312

313

314

Fig 6 a, b, c. Recurrence plots of waiting times of EQs in local seismicity from the March 1974 to the March 2017 for R=50 km (a) and water level in the Enguri dam reservoir from the Apr 1978 to August 2017, where on the axes are day marks after the start of recharge. The blue cells correspond to a less recurrence and yellow ones – to better recurrence of events; (c) the DFA analysis reveals beginning of ordering in seismic events after 1980 and strong recurrence regime after 1986.

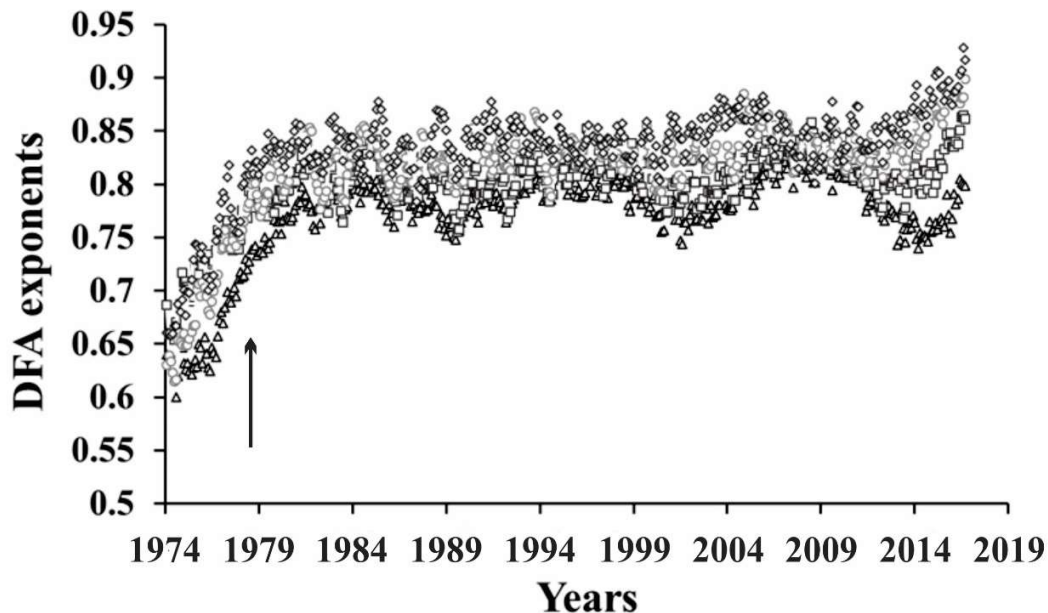
The distinct transitions from less regular to more regular pattern in seismic regime occur in 1985-1986 (a), when the WL change in reservoir became quasiperiodic, i.e. at the day mark 2000 in

315 Fig. 6b, which corresponds to the year 1985 (b); see also Fig. 3. Note light yellow diagonal lines in
316 (a) after 1986, which is a mark of quasi-periodicity in RIS. Similarly, the DFA analysis (Fig. 6c) points
317 to beginning of ordering in seismic events after 1980 and transition to strong recurrence regime after
318 1986.

319 *Results for M2.2 the far zone R=100 km.* We used DFA, RP, RQA and LZC methods for
320 interevent and magnitude data sequences from Enguri seismic catalogue (1974-2017) involving 913
321 events above M2.2 occurred within 100 km distance from the dam.

322 In Fig. 7, we present results of DFA exponent α calculation of waiting time sequences.
323 Calculation was done for 500 data length windows shifted by 1 data. DFA exponents for interevent
324 times (Fig. 7) indicates gradual DFA exponent increase toward the period of reservoir water level
325 periodic variation. Stronger increase took place in period starting from the 1984 and lasts till 2017.
326 According to these results under influence of water level periodic variation in reservoir, long-range
327 correlation clearly increased in earthquakes time distribution while earthquakes magnitude
328 distribution is characterized by slight or negligible changes in a long-range features just at the
329 beginning of observation period and after 200th window. The DFA for earthquakes magnitude
330 distribution is characterized by slight or negligible changes in a long-range features.

331



332

333

334 Fig. 7. DFA exponents of waiting times' sequences (M2.2 threshold) around Enguri reservoir
 335 (100km) 1974-2017. Polynomial fit from 2 to 5. (triangles P=2, squares p=3, circles p=4, diamonds
 336 p=5). Arrow marks the beginning of lake recharge; long-range correlation increases after 1984.

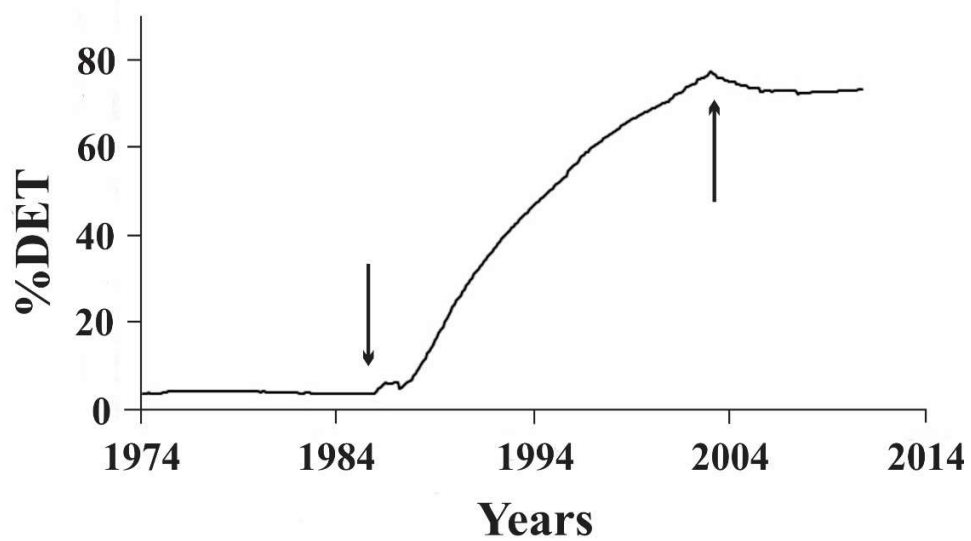
337

338 We applied also RQA and LZC methods to waiting times and magnitude data sequences
 339 from the Enguri seismic catalogue (1974-2017). Calculation was done for 500 data length windows
 340 shifted by 1 data.



341

342 Fig 8. %DET of magnitude data sequences (M2.2 threshold) around Enguri reservoir (R=100km)
 343 1974-2017. Note increased determinism in waiting times after 1986.

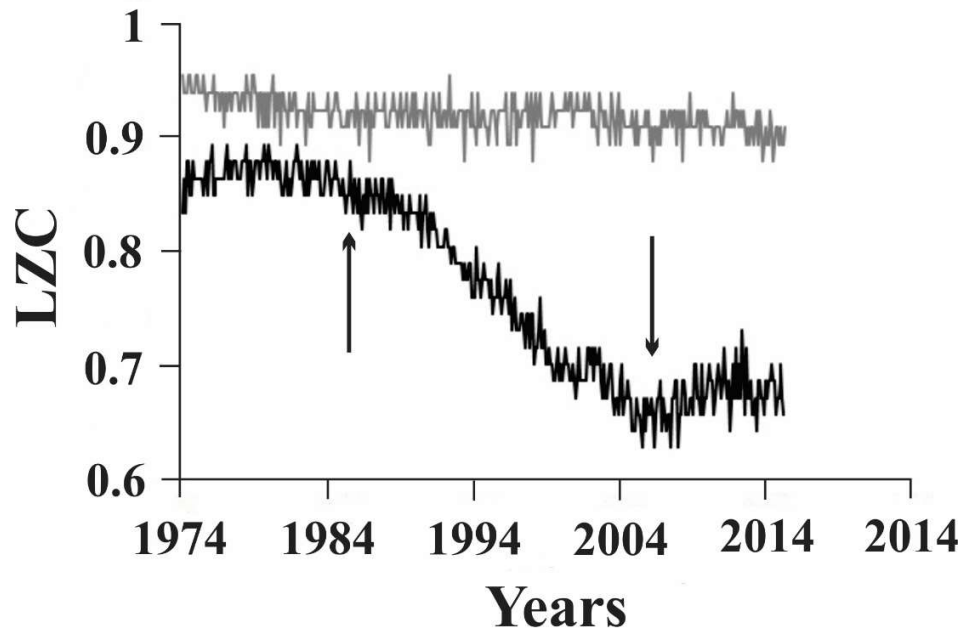


344

345

346 Fig. 9. %DET of interevent times sequences (M2.2 threshold) around Enguri reservoir (R=100km)
347 1974-2017. Note increased determinism in waiting times after 1986.

348



349

350 Fig. 10. Lempel and Ziv complexity measure calculated for (M2.2 threshold) around Enguri
351 reservoir (R=100km) 1974-2017 using 500 data windows shifted by 1 data. Magnitudes sequence
352 (grey) and interevent sequence (black).

353 **5. Discussion: Nonlinear dynamics patterns in seismicity and water level variations in** 354 **Enguri lake.**

355 Let us consider results, obtained by different complexity analysis approaches: the methods
356 abbreviation with a subscript m for magnitude time series and for the waiting times – by a subscript
357 wt : for example, accordingly $(RQA)_m$ and $(RQA)_{wt}$.

358 i. We can elucidate the transition in seismic regime by $(DFA)_{wt}$ the intensive increase of the
359 DFA exponent for the waiting times after 1984.

360 ii. Using RQA approach we reveal drastic changes in ETS dynamics for $(\%DET)_m$ after 1986
361 and for $(\%DET)_{wt}$ around 1986 and 2004, when the waiting times became maximal and stable.

362 iii. Using LZC we see that there are no changes in $(LZC)_m$, but $(LZC)_{wt}$ undergoes drastic
363 changes in waiting times dynamics around 1986 and 2004.

364 Resuming, we can mark the dates of significant changes in the seismic time series dynamics
365 around 1986 and in 2004 by both RQA and LZC methods.

366 Results of calculations presented in Fig. 6-10, convinces us that changes occurred in waiting
367 times data sets are much stronger than in magnitude sequences. At the same time %DET of waiting
368 times' sequence essentially increases and LZC noticeably decreases: both these effects point to the
369 growth of order (recurrence) in ETS in the period 1985-1986. According to these results under
370 influence of water level periodic variation in reservoir, long-range correlation clearly increased in
371 earthquakes time distribution, while earthquakes magnitude distribution is characterized by slight or
372 negligible change in long-range features.

373 Comparing dates of WL regime change and fault zone deformation patterns with transitions
374 in the ETS dynamics, we can conclude, that the transition in RQA and LZC in 1984-1986 is connected
375 with the beginning of the quasiperiodic load-unload process of the reservoir (see Fig. 3). Note, that
376 from 1985-1986 the strain in the fault zone under Enguri Dam also reveals quasi-periodic decoration
377 of the summary strain line (Fig. 3).

378 Thus, in the last period, beginning from the 1985-1986, the dynamics of local seismicity,
379 especially, waiting times is much more ordered due probably to synchronization of seismic activity
380 with WL variation regular pattern. This conclusion is confirmed by our earlier work where we carried
381 out analysis of Enguri area seismic activity using the Singular Spectrum Analysis (SSA) technique in
382 order to investigate the relationship of local seismicity with the reservoir water variations
383 (Matcharashvili et al, 2008; Matcharashvili et al, 2010; Telesca et al; 2012; Telesca, Chelidze, 2018).
384 We revealed the dominant one-year period in seismicity, which corresponds to seasonal load-unload
385 of the Enguri dam lake: this period was absent in ETS of the area in the reference period before lake
386 impoundment.

387 **Conclusions**

388 On the basis of the Recurrent Plots, Recurrent Quantification Analysis and Lempel-Ziv
389 Complexity analysis carried out on interevent and magnitude sequences of Enguri area seismic
390 catalogue, we conclude that influence of water level periodic variation makes time distribution of
391 local earthquakes more regular (synchronized with water level variation) comparing to the period
392 without such weak periodic influences. This means that nonlinear dynamics methods are effective in
393 detection and quantitative analysis of Reservoir Induced Seismicity near large dams as they make
394 possible to divide events, ordered by the impact of reservoir water regular strain from the
395 background seismicity.

396

397

398

399

400 **References**

401

402 Abashidze, V. Geophysical Monitoring of Geodynamical Processes at Enguri Dam. Publishing
403 House Metsniereba, Tbilisi, 2001, (in Russian).

404 Aboy, M., Hornero, R., Abásolo, D. and Álvarez, D., (2006) Interpretation of the Lempel-Ziv
405 complexity measure in the context of biomedical signal analysis, IEEE Trans. Biomed. Eng.,
406 53(11), 2282–2288.

407 Balavadze, B. (Ed). Geological-geophysical studies in the region of Enguri Hydro power station.
408 Publishing House “Metsniereba”, 1981, Tbilisi (In Russian).

409 Chelidze, T., Matcharashvili, T., Abashidze, V., Kalabegashvili, M., Zhukova, N. (2013). Real time
410 monitoring for analysis of dam stability: Potential of nonlinear elasticity and nonlinear
411 dynamics approaches. Front. Struct. Civ. Eng. 7:188-205, doi: 10.1007/s11709-013-0199-5.

412
413 Chelidze, T., Valliantos, F., Telesca, L., Eds. (2018) Complexity of seismic time series:
414 Measurement and Applications. Elsevier, Amsterdam.

415

416 Cover, T. and Thomas J. *Elements of Information Theory*. New York: Wiley, 1991.

417 Eckmann, J. P., Kamphorst, S., Ruelle, D. (1987), Recurrence plots of dynamical systems,
418 Europhysics Letters. 4, 973-977.

419 Foulger G., Miles P., Wilson M., Gluyas, J., Juliana, B., Davies, R. (2017), Global review of human-
420 induced earthquakes. Earth-Sci. Rev. doi.org/10.1016/j.earscirev.2017.07.008

421 Gamkrelidze, I., Giorgobiani, T., Kuloshvili, S., Lobzhanidze, G., Shengelaia, G. 1998. Active Deep
422 Faults Map and Catalogue for the Territory of Georgia, Bulletin of the Georgian Academy of
423 Sciences. 157(1), 80-85.

424 Grigoli, F., S. Cesca, E. Priolo, A. P. Rinaldi, J. F. Clinton, T. A. Stabile, B. Dost, M. G. Fernandez,
425 S. Wiemer, and T. Dahm. (2017). Current challenges in monitoring, discrimination, and
426 management of induced seismicity related to underground industrial activities: A European
427 perspective, *Rev. Geophys.*, 55, doi:10.1002/2016RG000542.

428
429 Gupta, H. K. 1992. Reservoir-Induced Earthquakes, Elsevier, Amsterdam, The Netherlands.
430
431 Gupta H. K. 2018. Review: Reservoir Triggered Seismicity (RTS) at Koyna, India, over the Past 50
432 Yrs. Bulletin of the Seismological Society of America, Vol. 108, No. 5B, pp. 2907–2918,
433 doi: 10.1785/0120180019

434 Hu, J., Gao, J., 2006. Analysis of Biomedical Signals by the Lempel-Ziv Complexity: the Effect of
435 Finite Data Size, *IEEE Trans Biomed Eng.* 53, pp. 2606-2609.

436 Kafka, A., John, E. (2011). Proximity to Past Earthquakes as a Least-Astonishing Hypothesis for
437 Forecasting Locations of Future Earthquakes. *Bull. Seis.Soc.America*, 101, 1618–1629,
438 doi: 10.1785/0120090164.

439 Lempel A. and Ziv, J. 1976. “On the complexity of finite sequences,” *IEEE Trans. Inf. Theory*, vol.
440 IT-22, no. 1, pp. 75–81, Jan.

441 Marwan, N., Romano, M. C., Thiel, M., Kurths, J. (2007), Recurrence plots for the analysis of
442 complex system, *Phys. Rep.* 438, 237–329.

443
444 Matcharashvili, T., Chelidze, T., Peinke, J. (2008). Increase of order in seismic processes around
445 reservoir induced by water level periodic variation. *Nonlin. Dyn.* 51: pp 399–407.

446 Matcharashvili, T., Chelidze, T., Abashidze, V., Zhukova N., Mepharidze, E. 2010. Changes in
447 Dynamics of Seismic Processes Around Enguri High Dam Reservoir Induced by Periodic
448 Variation of Water Level. in: *Geoplanet: Earth and Planetary Sciences*, Volume 1, 2010,
449 DOI: 10.1007/978-3-642-12300-9; Synchronization and Triggering: from Fracture to
450 Earthquake Processes. Eds.V.de Rubeis, Z. Czechowski and R. Teisseyre, pp.273-286

451 Peng, C.K., Buldyrev, S. V., Havlin, S., Simons, M., Stanley, H. E., and Goldberger, A. L., 1994.
452 Mosaic organization of DNA nucleotides, *Phys. Rev. E*, 49, 1685–1689,
453 doi:10.1103/PhysRevE.49.1685,

- 454 Peng, C.K., Havlin, S., Stanley, H., Goldberger, A. (1995). Quantification of scaling exponents and
455 crossover phenomena in nonstationary heartbeat time series, *Chaos*, 5, 82–87,
456 doi:10.1063/1.166141.
- 457 Savage, H., Kirkpatrick, J., Mori, J., Brodsky, E., Ellsworth, W., Carpenter, B., Chen, X., Cappa, F.,
458 Kano, Y. (2017) Scientific Exploration of Induced Seismicity and Stress (SEISMS). *Sci.*
459 *Dril.*, 23, 57–63, <https://doi.org/10.5194/sd-23-57-2017>.
- 460 Telesca, L., Chelidze, T. (2018) Visibility graph analysis of seismicity around Enguri
461 high arch dam, Caucasus. *Bull. Seis. Soc. America*, 108, doi: 10.1785/0120170370.
- 462 Telesca, L., Matcharashvili, T., Chelidze, T., Zhukova, N. (2012). Relationship between seismicity
463 and water level in the Enguri high dam area (Georgia) using the singular spectrum
464 analysis. *Nat. Hazards Earth Syst. Sci.*, 12, doi:10.5194/nhess-12-2479-2012
- 465 Webber, C. L., and Zbilut, J. P. (1994), Dynamical assessment of physiological systems and states
466 using recurrence plot strategies, *J. Appl. Physiol.* 76, 965–973.
- 467 Webber, C. L., and Zbilut, J. P., (2005). Recurrence quantification analysis of nonlinear dynamical
468 systems, In: *Tutorials in contemporary nonlinear methods for the behavioral sciences* (ed.
469 Riley M. A. and Van Orden G. C), pp. 26–94.
- 470 Webber, C.L., Marwan, N., Facchini, A., Giuliani, A. (2009). Simpler methods do it better: Success
471 of Recurrence Quantification Analysis as a general purpose data analysis tool, *Physics*
472 *Letters A* 373, 3753–3756.
- 473 Webber, C. and Marwan, N., Eds. (2015). *Recurrence Quantification Analysis: Theory and Best*
474 *Practices*, Springer Cham Heidelberg.
- 475 Zbilut, J. P., and Webber, C. L. (1992), Embeddings and delays as derived from quantification of
476 recurrence plots, *Phys. Lett. A* 171, 199–203.
- 477
478
479 Corresponding author: Tamaz Chelidze; tamaz.chelidze@gmail.com